



1 **Variations of atmospheric PAHs concentrations, sources, health risk, and direct**
2 **medical costs of lung cancer around the Bohai Sea under the background of**
3 **pollution prevention and control in China**

4

5 Wenwen Ma^{1,4,5}, Rong Sun^{1,4,*}, Xiaoping Wang³, Zheng Zong^{1,4}, Shizhen Zhao², Zeyu Sun^{1,4,5},
6 Chongguo Tian^{1,4,*}, Jianhui Tang^{1,4}, Song Cui⁶, Jun Li², Gan Zhang²

7

8 ¹ CAS Key Laboratory of Coastal Environmental Processes and Ecological Remediation, Yantai
9 Institute of Coastal Zone Research, Chinese Academy of Sciences, Yantai Shandong 264003, P.R.
10 China

11 ² State Key Laboratory of Organic Geochemistry, Guangzhou Institute of Geochemistry, Chinese
12 Academy of Sciences, Guangzhou, 510640, China

13 ³ Ludong University, Yantai, 264025, China

14 ⁴ Shandong Key Laboratory of Coastal Environmental Processes, Yantai Shandong 264003, P.R.
15 China

16 ⁵ University of Chinese Academy of Sciences, Beijing, 100049, China

17 ⁶ International Joint Research Center for Persistent Toxic Substances (IJRC-PTS), School of Water
18 Conservancy and Civil Engineering, Northeast Agricultural University, Harbin 150030, China

19

20 * Correspondence to: Rong Sun (rsun@yic.ac.cn) and Chongguo Tian (cgtian@yic.ac.cn)

21



22 **Abstract.** The Bohai Sea (BS) as the most polluted area of PAHs in China has been received wide
23 attention in recent decades. To characterize the variations of concentrations and sources of PAHs
24 from June 2014 to May 2019, fifteen congeners of PAHs ($\sum_{15}\text{PAHs}$) were measured from
25 atmospheric samples (N=228) collected at 12 sites around the BS, and health risk and direct
26 medical costs associated with lung cancer exposed to PAHs were also estimated. The annual daily
27 average concentration of $\sum_{15}\text{PAHs}$ was $56.8 \pm 4.7 \text{ ng m}^{-3}$, dominated by low molecular weight
28 (LMW-PAHs, 3-ring) ($58.9 \pm 7.8\%$). During the five-year sampling period, the atmospheric
29 $\sum_{15}\text{PAHs}$ concentration reduced by 17.5% for the whole BS, especially in the tightly controlled
30 area of Tianjin (TJ) with a drop of 51.7%, which was mainly due to the decrease of high molecular
31 weight PAHs (HMW-PAHs, 5-6 ring) concentration. Generally, the concentration of $\sum_{15}\text{PAHs}$ was
32 highest in winter and lowest in summer, mainly attributed to the change of LMW-PAHs
33 concentration. Based on PMF model, PAHs at the BS were mainly ascribed to coal combustion and
34 biomass burning. And the contribution of coal combustion and motor vehicle to PAHs had a
35 different performance between the BS (coal combustion rose by 6.7%, motor vehicle fell by 22.7%)
36 and TJ (coal combustion fell by 13.2%, motor vehicle rose by 6.7%). The incidence of lung cancer
37 (ILCR) caused by exposing to atmospheric PAHs at the BS and TJ decreased by 74.1% and 91.6%
38 from 2014 to 2018, respectively. That was mainly due to the decrease of the concentration of highly
39 toxic HMW-PAHs. It was reflected on the savings of \$10.7 million in direct medical costs of lung
40 cancer exposed PAHs, which was accounted 46.1% before air prevention and control around the
41 BS. And there was a higher cost reduction of 54.5% in TJ. Hence, this study proved that
42 implementing pollution prevention and control not only effectively reduced the concentration of
43 pollutants and the caused risks, but also significantly reduced the medical costs of diseases caused
44 by corresponding expose.

45



46 **1 Introduction**

47 Polycyclic aromatic hydrocarbons (PAHs) were a class of classical organic compounds with
48 at least two benzene rings, and have been received long-term attention because of cytotoxic,
49 teratogenic, mutagenic, or carcinogenic (Colvin et al., 2020; Marvin et al., 2020). The United States
50 Environmental Protection Agency (USEPA) identified sixteen PAH congeners as priority pollutants
51 (Lv et al., 2020). The sixteen PAH congeners in the atmosphere were considered as a major portion
52 of lung cancer risk to the public because of their relatively high concentration, strong toxic potency,
53 and long-term distance transmission (Ma et al., 2010; Gong et al., 2011; Ma et al., 2013; Hong et
54 al., 2016). According to the statistics, the incidence and mortality of lung cancer were ranked first
55 among cancer-related cases in the world, and so the lung cancer risk owing to exposing to PAHs
56 was of particular concern and widely assessed (Jia et al., 2011; Zhuo et al., 2017; Lian et al., 2021).

57 PAHs were emitted primarily via incomplete combustion and pyrolysis of carbon-contained
58 materials, such as fossil fuels and biomass (Biache et al., 2014). China has been assessed as the
59 largest emitter of PAHs all over the world for recent two decade because of rapid development of
60 the economy and increasing consumption of carbon-contained materials (Zhang et al., 2007).
61 Beijing-Tianjin-Hebei (BTH) region was one of the regions with the highest PAHs emission
62 intensity and the heaviest atmospheric PAHs concentrations in China (Zhang et al., 2007; Zhang et
63 al., 2016). In such serious pollution, the health risk exposed to PAHs caused great concern. The
64 population attributable fraction (PAF) for lung cancer caused by inhalation of PAHs in the
65 atmosphere of the BTH area was more than twice higher than the mean value in whole China in
66 2009 (Zhang et al., 2009). The incremental lifetime cancer risk (ILCR) of the PAHs exposure at
67 Tianjin was in the range of 1×10^{-5} to 1×10^{-3} in 2008, which was much higher than the mean level
68 of 4.56×10^{-6} in China (Lian et al., 2021; Bai et al., 2009). The annual lung cancer morbidity of
69 Tianjin (6.99×10^{-6}) within the BTH region was the highest city among 35 cancer registries in
70 China (Zhang et al., 2007). Meanwhile, with the frequent occurrence of haze in the BTH region,
71 more attention has been paid to concentration levels and health risk of fine particulate matter with
72 aerodynamic equivalent diameter $\leq 2.5 \mu\text{m}$ ($\text{PM}_{2.5}$) since 2013 (Chen et al., 2020).



73 PM_{2.5} pollution in China has obviously been improved since the Air Pollution Prevention and
74 Control Action Plan (2013-2017) and the Three-year Action Plan for Winning the Blue-Sky
75 Defense Battle (2018-2020) were proposed by the Chinese government in 2013 and 2018 (Zhao et
76 al., 2023). As the most severely polluted area in China, the improvement was more significantly at
77 the BTH region, which implemented the strictest pollution control policy (Li et al., 2020). As
78 reported that the concentration of PM_{2.5} at the BTH region dropped by 52% from 106 µg m⁻³ in
79 2013 to 51 µg m⁻³ in 2020 (Bulletin of the State of China's ecological Environment, 2021). In the
80 prevention and control of pollution policies, reducing emissions of coal combustion and motor
81 vehicle were the major parts (Guo et al., 2018; Li et al., 2019). The two sources have been
82 recognized as primary contributors to PAHs in the atmosphere as well (Lin et al., 2015; Han et al.,
83 2018). As a result, the controls of the two sources not only reduced PM_{2.5} emission, but also PAHs
84 emission (Zhi et al., 2017). During the controlling processes, the variations in the concentrations
85 and health risk of PM_{2.5} at BTH region have been well identified (Fang et al., 2016; Yan et al.,
86 2019), while the relevant understanding of PAHs in the region urgently needs to be updated.
87 Especially, the statistical data of the lung cancer risk due to exposing to PAHs was established ten
88 years ago (Zhang et al., 2009; Bai et al., 2009).

89 To track changes in concentrations and source of atmospheric PAHs and estimate health risk
90 and the direct medical costs associated with lung cancer by exposing to PAHs during the air
91 pollution control actions, a field monitoring campaign was conducted at twelve sites around the BS
92 for five years from June 2014 to May 2019. The BS is the only inland sea in China, and surrounded
93 by the BTH region, the Liaodong Peninsula, and the Shandong Peninsula (Liu et al., 2020). The
94 measures for air pollution control implemented were different at the BTH region, the Liaodong
95 Peninsula, and the Shandong Peninsula (Huang et al., 2017). Thus, it would provide us an
96 opportunity to understand the difference in environmental concentrations, source contributions, and
97 health risk of PAHs. The main aims of this study were (1) to characterize the spatial and temporal
98 changes of the concentrations and components of PAHs in the atmosphere around the BS, (2) to
99 evaluate the difference of source contributions of PAHs, and (3) to assess the changes of direct



100 medical costs for treating lung cancer caused by inhalation exposure to PAHs under atmospheric
101 prevention and control in the five years.

102 **2 Materials and methods**

103 **2.1 Sampling site and sample collection**

104 The sampling sites for this study had been reported in previous literatures (Sun et al., 2021),
105 and it was briefly introduced here. The information of the sites was shown in Table S1 of the
106 Supporting Information (SI). Twelve air sampling sites were located at Beihuangcheng (BH),
107 Dalian (DL), Donggang (DG), Dongying (DY), Gaizhou (GZ), Longkou (LK), Laoting (LT),
108 Rongcheng (RC), Tianjin (TJ), Xingcheng (XC), Yantai (YT), and Zhuanghe (ZH). A passive air
109 sampler with polyurethane foam (PUF, 14 cm diameter × 1.35 cm thickness) was used to collect
110 atmospheric samples at each sampling site (Eng et al., 2014). The PUF disks were deployed around
111 1.5–2.0 m above the ground, the sampling duration was about 3 months for one batch. 228 samples
112 were collected from June 2014 to May 2019. The sampling rate of atmospheric PAHs was 3.5 m³
113 day⁻¹ (Jaward et al., 2005; Moeckel et al., 2009). Prior to sampling, the PUF disks were pre-cleaned
114 by methanol, acetone, and hexane, respectively. The extracted PUF disks were placed in airtight
115 containers and stored at –18 °C before the sampling campaign. After sampling, the samples were
116 prepared and then stored at a –18 °C freezer in the lab for further analyses.

117 **2.2 Sample pretreatment and instrumental analysis**

118 The five PAHs surrogates (Naphthalene-*D*₈, Acenaphthene-*D*₁₀, Phenanthrene-*D*₁₀, Chrysene-
119 *D*₁₂, Perylene-*D*₁₂) and the activated copper fragments were added in advance (Qu et al., 2022).
120 The samples were extracted for 24 h, which the elution was acetone and hexane (200mL, v:v=1:1)
121 through Soxhlet apparatus. The extracted solution was concentrated to 1mL with rotary evaporator
122 (SHB-III, Zhengzhou Greatwall Ltd., China). Then, silica-alumina column was used to obtain the
123 aromatic components, then the targets were obtained with 40 mL of a mixed solution of
124 dichloromethane and hexane (v:v=1:1). Finally, the eluent was concentrated and reduced to 500 μL
125 by a gentle nitrogen stream. As the internal standard substance, 400 ng of hexamethylbenzene
126 (Supelco, USA) was added to each sample solution before the instrumental analysis.



127 The targets were detected through the gas chromatograph equipped with mass spectrometry
128 (GC-MS, Agilent 5975C-7890A, USA), and the chromatographic column was DB-5MS (Agilent
129 Technologies, 30 m × 0.25 mm × 0.25 μm). Each extract was injected by 1 μL with splitless mode.
130 High-purity helium (purity ≥ 99.99%) with a flow rate of 1.3 mL min⁻¹ was used as the carrier gas.
131 The process of oven temperature was set as at 80 °C with a hold of 3 minutes, and then raised to
132 310 °C by 10 °C min⁻¹, and then hold 10 minutes. The temperatures of inlet and ion source were
133 290 °C and 230 °C, respectively. The details of the targeted compounds were shown in Table S2 of
134 SI. Seven gradients of mixed solutions were established for quantitative calculation of PAHs. More
135 details were reported in previous study (Wang et al., 2018).

136 **2.3 Quality assurance and quality control**

137 The mean recovery values of Naphthalene-D₈, Acenaphthene-D₁₀, Phenanthrene-D₁₀, Chrysene-
138 D₁₂, and Perylene-D₁₂ were 77.3%, 85.9%, 87.5%, 88.3%, and 92.8%, respectively, which were
139 ranging from 66.5% to 123.1%. All the relative deviations were within 20%, except for
140 Naphthalene-D₈. Nap was excluded because of its low recovery, and the other fifteen PAHs
141 (Σ₁₅PAHs) were used for further discussion in this study. For each batch of twelve PUF samples, a
142 field blank and a procedural blank were also analyzed at same treatment process. In this study, the
143 method detection Limits (MDLs, defined as the mean blank value plus 3 times the standard
144 deviation) for 15 PAH congeners ranged from 0.016 to 0.126 ng sample⁻¹, which were shown in
145 Table S2 of SI. The final concentrations were not surrogate-corrected. The glassware was all
146 cleaned and burned for 8 hours in muffle oven at 450 °C before the experiment. The solvents were
147 chromatography-pure or had been redistilled and purified before using.

148 **2.4 Source apportionment of PAHs**

149 The model of positive matrix factorization (PMF) released by the USEPA (PMF 5.0) was used
150 to apportion the emission sources of PAHs in this study. The basic calculation formula of the PMF
151 method is as Eq. (1):

$$152 \quad x_{ij} = \sum_{k=1}^p g_{ik} \cdot f_{kj} + e_{ij} \quad (1)$$



153 where p represents the number of sources identified by the PMF model. x_{ij} represents original
154 concentration data of i^{th} chemical species and j^{th} sample. f_{ik} represents the source profile of k^{th}
155 source and j^{th} chemical species. g_{kj} represents contribution ratio of k^{th} source to j^{th} sample. e_{ij}
156 represents the simulated residual error of i^{th} chemical species and j^{th} sample. Source contributions
157 and profiles are solved by the PMF model minimizing the objective function Q , as Eq. (2):

$$158 \quad Q_{\min} = \sum_{i=1}^n \sum_{j=1}^m \left(\frac{x_{ij} - \sum_{k=1}^p g_{ik} f_{kj}}{u_{ij}} \right)^2 \quad (2)$$

159 where x_{ij} , g_{ik} , and f_{kj} are same that in Eq. (1), respectively. u_{ij} is the uncertainty of x_{ij} , and the
160 calculation method of uncertainty is showed in Text S2 of SI. More details have been documented
161 (Sofowote et al., 2011; Paatero et al., 2014).

162 Before the source apportionment, principal component analysis (PCA) was applied to pre-
163 estimate the minimum number of emission sources in this study because PCA was able to explain
164 the overall variables with fewer variables with a minimum loss of information (Liu et al., 2021).
165 SPSS Statistics 25.0 was used to perform the PCA analysis in this study.

166 2.5 Health risk assessment

167 The total toxicity equivalent (TEQ , ng m^{-3}) of the fifteen PAHs with BaP as reference is
168 calculated as Eq. (3):

$$169 \quad TEQ = \sum_{i=1}^n (C_i \times TEF_i) \quad (3)$$

170 where C_i is concentration of the i^{th} PAH compound (ng m^{-3}), TEF_i is the cancer potency of the
171 i^{th} PAH compound (dimensionless), as shown in Table S2 of SI.

172 $ILCR$ in this study referred to cancer risk in a population due to exposure to a specific
173 carcinogen (Zhuo et al., 2017). Its calculation formula is as Eq. (4):

$$174 \quad ILCR = UR_{BaP} \times TEQ \quad (4)$$

175 In above, UR_{BaP} represents the cancer risk when the concentration of BaP is 1 ng m^{-3} (ng m^{-3}).
176 According to the regulations of World Health Organization (WHO), UR_{BaP} can be 8.7×10^{-5} per



177 ng m⁻³. That is, in terms of life span of 70 years, lifetime exposure to *BaP* concentration of 1 ng m⁻³
178 ³ resulted in a risk of cancer by inhalation of 8.7×10^{-5} (Luo et al., 2021).

179 **2.6 Medical costs assessment**

180 In this study, the medical costs were assessed by comparing total direct medical costs for
181 treating lung cancer caused by respiratory exposed to PAHs in the atmosphere under the assumption
182 that no air pollution control and the actual implementation of air pollution control. The total direct
183 medical costs for treating lung cancer (C_t) are calculated as Eq. (5):

$$184 \quad C_t = C_{pc} \times P \times I_{add} \quad (5)$$

185 where C_t is the total direct medical costs of lung cancer induced by PAHs exposure, C_{pc} is the
186 per capita direct medical costs of lung cancer, and a cost of \$8,700 in China in 2014 was used in
187 this study (Shi et al., 2017). P is the annual population, I_{add} is the additional incidence of lung cancer
188 due to PAHs inhalation exposure, it is calculated as Eq. (6):

$$189 \quad I_{add} = I \times PAF \quad (6)$$

190 where I is the incidence of lung cancer. And the I value was 87.37×10^{-5} at Tianjin estimated
191 in 2012, which was referred in this study (Cao et al., 2016). PAF is the population attributable
192 fraction, defined as the decrease in the incidence or mortality of a disease when a certain risk factor
193 is completely removed or reduced to another lower reference level (Menzler et al., 2008). The PAF
194 can be calculated as Eq. (7):

$$195 \quad PAF = \frac{rr(TEQ) - 1}{rr(TEQ)} \quad \text{and} \quad rr(TEQ) = [URR_{cum, exp = 100}]^{(TEQ \times 70 / 100)} \quad (7)$$

196 where rr is relative risk, that is, the risk of exposure to a specific concentration relative to no
197 exposure. URR is the unit relative risk, a reference value of 4.49 per 100 $\mu\text{g m}^{-3}$ years of *BaP*
198 exposure was adopted in this study (Zhang et al., 2009). This reference value was based on an
199 epidemiological study on lung cancer conducted in Xuanwei, China (Menzler et al., 2008) (Gibbs
200 et al., 1997). This study assumed that the mean life expectancy in China was 70 years, and the
201 lifetime exposure was equivalent to 70 years.

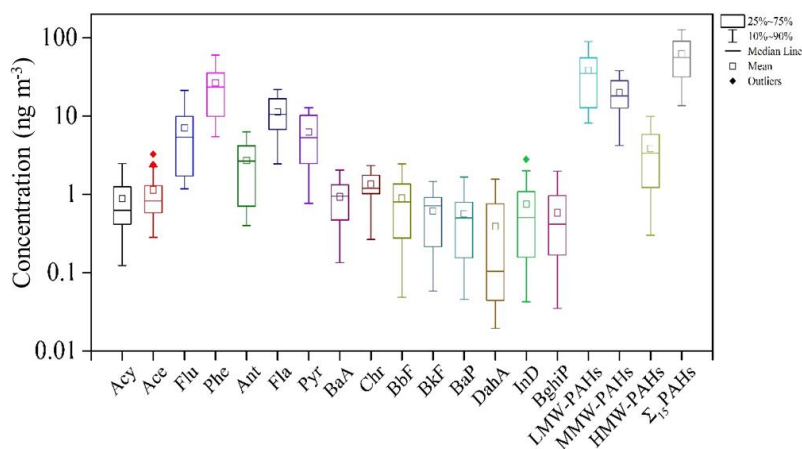
202 **3 Results and discussions**



203 3.1 Concentration and composition of PAHs

204 3.1.1 General information of PAHs

205 Figure 1 summarizes the annual daily average concentrations of 15 PAHs in the atmosphere
206 at the twelve sampling sites around the BS from June 2014 to May 2019. The annual daily average
207 concentration of Σ_{15} PAHs around the BS was $56.8 \pm 4.7 \text{ ng m}^{-3}$, with a range of 51.4 – 63.6 ng m^{-3} .
208 ³. And the highest concentration was the low molecular weight PAHs (LMW-PAHs, 3-ring),
209 followed by middle molecular weight PAHs (MMW-PAHs, 4-ring) and high molecular weight
210 PAHs (HMW-PAHs, 5-ring and 6-ring), which were accounting for 58.7%, 34.8%, and 6.65% of
211 the total concentration, respectively. The atmospheric PAHs concentration was dominated by the
212 LMW-PAHs in this study, which Phe, Fla, and Flu were the main compounds accounting for 37.7%,
213 19.8%, and 12.6% of the total. The atmospheric PAHs concentrations around the BS were at a
214 higher pollution level than the Yangtze River Delta and the Pearl River Delta, such as Ningbo (45
215 ng m^{-3}) (Tong et al., 2019) and Guangzhou (9.72 ng m^{-3}) (Yu et al., 2016). And the atmospheric
216 concentrations of PAHs around the BS were also much higher than in atmosphere above the Great
217 Lakes (1.3 ng m^{-3}) (Li et al., 2021) and southern Europe cities (3.1 ng m^{-3}) (Alves et al., 2017).
218 Overall, it was found that the pollution of atmospheric PAHs around the BS was still worrying.
219





220 **Figure 1.** Atmospheric concentrations of PAHs around the BS from June 2014 to May 2019.

221

222 **3.1.2 Temporal variations of PAHs**

223 For seeking better understand the variation characteristics of PAHs in the atmosphere, the
224 summer of the previous year to the spring of the next year were taken as a statistical cycle. The
225 concentrations of Σ_{15} PAHs in the five annual cycles around the BS were $63.6 \pm 58.4 \text{ ng m}^{-3}$ (2014-
226 2015), $55.5 \pm 37.9 \text{ ng m}^{-3}$ (2015-2016), $60.9 \pm 31.1 \text{ ng m}^{-3}$, (2016-2017), $51.4 \pm 29.4 \text{ ng m}^{-3}$ (2017-
227 2018), and $52.5 \pm 40.1 \text{ ng m}^{-3}$ (2018-2019), respectively (Table S3 of SI). Overall, the
228 concentrations of Σ_{15} PAHs from June 2014 to May 2019 showed a slow downward trend with a
229 decrease of 17.5%. The decrease of atmospheric PAHs concentrations was mainly due to the
230 decline of the HMW-PAHs concentrations. The HMW-PAHs composition ratio decreased from
231 11.3% (2014-2015) to 3.44% (2018-2019), while the MMW-PAHs raised from 35.5% (2014-2015)
232 to 41.2% (2018-2019). The LMW-PAHs composition ratio was stable from 53.4% (2014-2015) to
233 55.4% (2018-2019). The one factor that effected the concentrations of PAHs in the atmosphere
234 after they were discharged from the emission source was meteorological conditions (Fan et al.,
235 2021), and the other important factor was the amount of the direct emission from the emission
236 source (Ma et al., 2018). The sources of PAHs with different ring numbers were different (Li et al.,
237 2021). LMW-PAHs were mainly produced in the combustion process of non-petroleum sources,
238 while HMW-PAHs were mainly from high temperature combustion products generated by fossil
239 fuel combustion, including some activities involving pyrolysis process, such as vehicle emissions,
240 industrial productions, and other high-temperature source emissions (Zhang et al., 2018; Xing et
241 al., 2020). The significant decrease of HMW-PAHs concentrations at the BS during the five-year
242 observation period might be related to the decrease of high temperature emission sources. Due to
243 the high toxicity characteristics of HMW-PAHs (Biache et al., 2014; Ma et al., 2020), the decrease
244 of its concentration might indicate a decrease in the environmental toxicity of PAHs.

245 The seasonal distributions of PAHs concentrations in the atmosphere of the BS region showed
246 high in cold season and low in warm season. The concentrations of Σ_{15} PAHs in four seasons were



247 as follow: winter ($104.3 \pm 9.50 \text{ ng m}^{-3}$) > autumn ($53.9 \pm 9.10 \text{ ng m}^{-3}$) > spring ($43.9 \pm 19.5 \text{ ng m}^{-3}$) > summer ($26.3 \pm 13.4 \text{ ng m}^{-3}$) (Table S5 of SI). The concentration of PAHs in winter was about
248 3) > summer ($26.3 \pm 13.4 \text{ ng m}^{-3}$) (Table S5 of SI). The concentration of PAHs in winter was about
249 4 times higher than that in summer, and the maximum and minimum of the annual daily average
250 concentrations at 12 sampling point mostly occurred in winter and summer. In addition, there were
251 significant differences between total PAHs concentration and different ring number concentrations
252 ($p < 0.05$, the difference level is shown in Table S6 of SI). The seasonal characteristics of PAHs
253 concentrations in this study were consistent with reported results in North China (Ma et al., 2017;
254 Zhang et al., 2019). Interestingly, it was that the difference of PAHs concentrations in four seasons
255 was mainly on account of LMW-PAHs. This indicated that there were other important pollution
256 sources for LMW-PAHs, followed by MMW-PAHs, which was significantly increasing in winter
257 at the BS region. Then identifying the source of LMW-PAHs was crucial for improving
258 environmental quality of the BS. Studies have shown that coal burning emissions and biomass
259 burning were the main sources of atmospheric PAHs in this region (Liu et al., 2019). For typical
260 northern families, the consumption of firewood burning and coal in winter was 1.5–2.0 times higher
261 than that in summer due to heating and other activities (Qin et al., 2007). As a result, PAHs
262 emissions in winter were at least 1.5 times higher than those in summer. In addition, due to the
263 migration characteristics of atmospheric PAHs, meteorological conditions such as temperature and
264 wind direction in different seasons would also affect the observed concentration (Tan et al., 2006).
265 And low temperature and inversion layer in winter were not conducive to atmospheric diffusion,
266 resulting in a relatively high concentration of PAHs in the atmosphere near the surface (Wang et
267 al., 2018).

268 **3.1.3 Spatial characteristics of PAHs**

269 Figure 2 and Table S7 of SI displays the distribution of the five-year mean concentrations of Σ_{15}
270 PAHs from June 2014 to May 2019 at the 12 sampling sites around the BS. The concentrations of
271 atmospheric Σ_{15} PAHs ranged from $25.9 \pm 6.4 \text{ ng m}^{-3}$ (RC) to $103.7 \pm 39.1 \text{ ng m}^{-3}$ (XC). The
272 concentrations of PAHs on the BS north coast were twice higher than at the BS south coast. PAHs
273 were a class of pollutants that can undergo long-range transport in the atmosphere (Wang et al.,

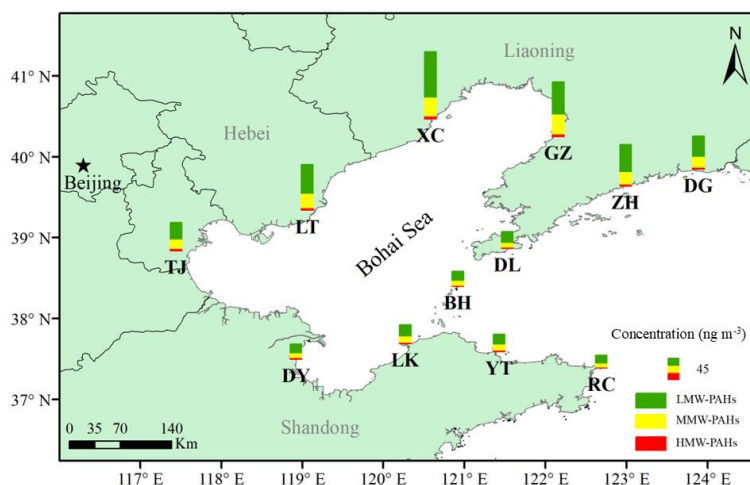


274 2018), and their spread was largely affected by local meteorological conditions (Ding et al., 2005).
275 The climate in North China and the adjacent oceanic area was greatly affected by the East Asian
276 monsoon, and the characteristic weather phenomenon in the winter monsoon was the strong north
277 and northwest winds (Tian et al., 2009). Due to the additional emissions from fuel consumption for
278 domestic heating in the source areas, the atmospheric PAHs concentrations significantly increased
279 (Feng et al., 2007; Gao et al., 2016). Combined with backward trajectory shown in Fig. S4 of SI, it
280 suggested that the elevated PAH concentrations in winter at the north of the BS were mainly
281 attributed to their outflow from the north and northwest source regions carried by the winter
282 monsoon winds. However, the composition of PAHs at the north-south showed consistency without
283 no significant differences (Table S8 of SI). As the whole, the composition of PAHs at 12 station
284 that the highest content was LMW-PAHs (North: 60.0%, South: 57.4%), followed by MMW-PAHs
285 (North: 32.7%, South: 32.4%), and HMW-PAHs was the lowest (North: 7.3%, South: 10.8%). The
286 above indicated that there were the same emission sources of PAHs in the atmosphere around the
287 BS.

288 However, for TJ, the study found that there was a more significant change in the concentration
289 of atmospheric PAHs, which decreased from 68.6 ng m^{-3} (2014-2015) to 33.1 ng m^{-3} (2018-2019).
290 The reason was mainly that TJ was located at the Beijing-Tianjin-Hebei region where was the
291 strictest area of air pollution prevention and control, as a key area in China's "12th Five Year Plan".
292 For exploring the potential differences of source emissions at 12 sampling points, Pearson
293 correlation analysis was used to analyze the seasonal distribution of PAHs concentrations as shown
294 in Table S9 of SI. Among the five stations (LK, DY, TJ, LT, and XC) at the western BS centered on
295 TJ, the correlation coefficients of atmospheric PAHs concentration (0.72–0.89) among the other
296 four stations were greater than that between each site and TJ (0.50–0.68). That the co-variability
297 of PAHs concentrations between TJ and the other four stations was weaker. This indicated that
298 there were certain differences between TJ's PAHs emission sources and adjacent areas.



299



300 **Figure 2.** The mean concentration distribution of Σ_{15} PAHs at 12 sites around the BS from June
301 2014 to May 2019.

302

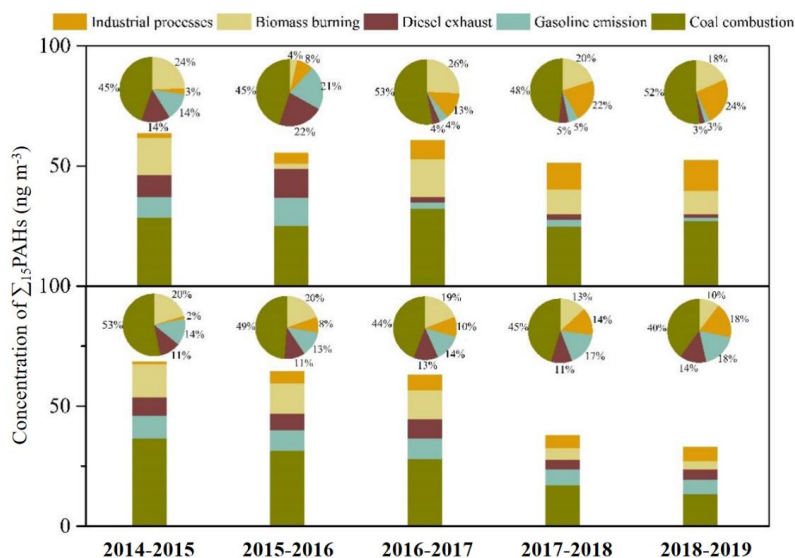
303 3.2 Source apportionment of PAHs

304 For further probing into the causes for the variations of the concentrations and compositions
305 of PAHs, the sources apportionment of PAHs in the atmosphere around the BS and TJ region from
306 2014-2015 to 2018-2019 was investigated via PCA and PMF. PCA analysis results showed that
307 when four factors (eigenvalues > 1) were extracted from the data set, the total cumulative load
308 accounted for more than 85% of the variance (Table S10 of SI). This indicated that at least four
309 types of emission sources could better explain the source of atmospheric PAHs. For PMF model,
310 the key process was to determine the correct number of factors, and this study was based on the
311 results of PCA. Based on the random seed, 4 – 7 factors were used through the PMF model for
312 source analytical simulation. The source analytical simulation of five factors determined the most
313 stable results and the most easily interpreted factors. The solution produces Q values (both robust
314 and true) that were close to the theoretical Q values, which was indicating that the PAHs data set
315 in the modeling input provided appropriate uncertainty. The data set used for PMF analysis



316 included the concentrations of 228 samples of 15 PAHs and uncertainties. The diagnostic regression
317 R^2 value for the overall concentrations of 15 PAHs components was 0.986. The predicted
318 concentrations of 15 PAHs via PMF model were almost consistent with the actual concentrations
319 of 15 PAHs around the BS (Fig. S5–S6 of SI and Text S2 of SI). It meant that the model results
320 were good and could be used as the judgment basis for source analysis of target species, so these 5
321 factors would well explain the source of PAHs. Contribution of source identified by PCA and PMF
322 were coal combustion, biomass burning, industrial processes, gasoline emission, and diesel
323 emission. The detailed information of source identification is shown Text S3 of SI.

324



325 **Figure 3.** Concentration and source contribution of Σ_{15} PAHs sources around the BS (the upper
326 part) and TJ (the lower part) from 2014-2015 to 2018-2019.

327

328 Fuel combustion emissions were the reason for the significant increase of atmospheric pollutants,
329 and that were also responsible for the elevated $PM_{2.5}$ levels around the BS region (Yang et al., 2017).
330 To explore the relationship between Σ_{15} PAHs and $PM_{2.5}$ concentrations, available online $PM_{2.5}$ data

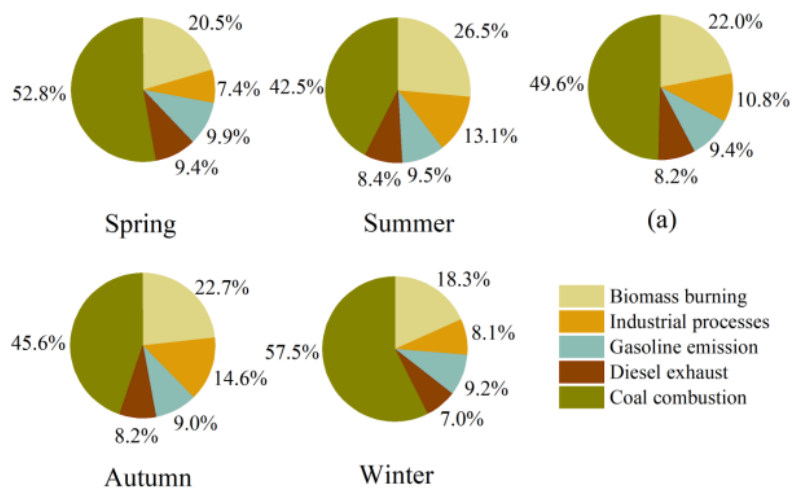


331 for eight cities that on behalf of sampling sites (DG, DL, DY, GZ, LT, TJ, XC, and YT) (Air quality
332 historical data query, 2014-2019) were collected, which averaged their concentrations according to
333 the sampling periods in the study (Table S12 of SI). The Pearson correlation coefficients of the
334 concentrations of atmospheric PAHs and PM_{2.5} were ranging from 0.485 to 0.868, and the
335 significant levels were greater than 95% as listed in Table S13 of SI. During the observation of the
336 five-year, the PM_{2.5} concentration at the BS region decreased by 29.6% from 57 μg m⁻³ to 40 μg m⁻³,
337 and at TJ showed an even greater decrease by 33.8% from 78 μg m⁻³ to 51 μg m⁻³. From 2013,
338 PM_{2.5} had been strictly controlled by the government year by year, which the significant correlation
339 indicated that the PAHs concentrations should be affected. To explore the potential influencing
340 factors of the difference in atmospheric PAHs composition between the BS area and TJ, their
341 average annual contributions of various PAHs emission sources from 2014-2015 to 2018-2019
342 were compared shown in Figure 3. During the sampling period of the BS region, coal combustion
343 was the main source of the atmospheric PAHs emission (45%), followed by biomass burning (24%)
344 in 2014-2015, which was switching to coal combustion (52%) and industrial processes (24%) in
345 2018-2019. For TJ, coal combustion was also the main source of the atmospheric PAHs emissions
346 (53%), followed by biomass burning (20%) in 2014-2015, which was switching to coal combustion
347 (40%), industrial processes (18%) and gasoline emissions (18%) in 2018-2019. The source
348 contributions of coal combustion to atmospheric PAHs had increased by 7% around the BS, while
349 the corresponding contributions in TJ had fallen by 13%. The absolute contribution (the total
350 concentration of PAHs multiplied by the percentage value of the contributing source) decreased,
351 which was indicating that the reduction of the coal contribution source had a significant
352 improvement on the atmospheric PAHs pollution.

353 The main source of atmospheric PAHs around the BS was coal combustion (Liu et al., 2019; Qu
354 et al., 2022), while for TJ, as one of the key areas for air pollution control in China, had taken
355 stricter measures to control emissions of coal combustion (Wu et al., 2015). For instance, the city
356 took the lead in the switching domestic fuel from coal to natural gas and electricity in 2017 to
357 reduce emissions of air pollutants (Zhang et al., 2021). These targeted measures had more



358 forcefully controlled coal-combustion emissions for PAHs in TJ than the other places around the
359 BS region (Guo et al., 2018). Vehicle emission (gasoline and diesel exhaust) to atmospheric PAHs
360 had experienced a sharp drop of 23% for the BS area, while for TJ risen by 7%. The same trend for
361 vehicle emission was found in the study of Beijing and Tianjin (Zhang et al., 2016; Chao et al.,
362 2019). The decrease was mainly due to the elimination and scrapping of substandard vehicles
363 carried out by the Chinese government in 2015. Based on the “China Vehicle Environmental
364 Management Annual Report”, the car ownership around the BS increased by about 17.5 million,
365 but the emissions of hydrocarbons including PAHs reduced by 95,000 tons from 2014 to 2018 (Fig.
366 S8 of SI). The source apportionment showed that the contribution of vehicle emission to PAHs had
367 a sharp decline since the spring of 2016 (Fig. S9 of SI), with a decreased by 38% (19% for gasoline
368 and 19% for diesel) around the BS (Huang et al., 2017). Although the contribution of vehicle
369 emissions for TJ was increased, the concentrations of PAHs was decreasing. It indicated that these
370 measures had also controlled vehicle emissions and kept the emissions of PAHs at a low level.
371 Therefore, targeted control measures could effectively control PM_{2.5} and PAHs pollution in the
372 atmosphere at the BS and TJ. Moreover, PAHs were a kind of organic compounds produced with
373 black carbon (BC), and, to some extent, the molecular characteristics of PAHs also provided the
374 basic data to analysis of the source of BC in the atmosphere of the BS (Fang et al., 2016). At the
375 same time, the PAHs source analysis results of this study revealed that the composition and source
376 of atmospheric BC in the BS region have also changed from 2014 to 2019. This problem needs our
377 attention and confirmation.



378

379 **Figure 4.** The seasonal and average contributions for five sources of Σ_{15} PAHs derived from PMF;
380 (a): the five-year average contributions of five sources.

381

382 Figure 4 shows the seasonal distribution of five sources for atmospheric PAHs at the BS.
383 Generally, the seasonal distribution of five sources for atmospheric PAHs at TJ was consistent with
384 that the BS, which was not separately discussed here. Coal combustion was the main emission
385 source in the four seasons, followed by biomass burning, while the contributions of the others
386 (industrial processes, gasoline emission, and diesel emission) were similar. Compared with other
387 seasons, the contribution of coal combustion for atmospheric PAHs to the BS was the highest in
388 winter, which was followed by spring, and the lowest was in summer. This was consistent with the
389 seasonal distributions of the concentrations of PAHs in the atmosphere at the BS. Based on the
390 seasonal distribution of concentrations, the increase concentrations of atmospheric PAHs in winter
391 were mainly caused by coal combustion. This might be due to people in cold winters at northern
392 China rely on coal combustion for heating. For biomass combustion, it was higher in summer and
393 autumn, which was related to straw burning after harvest. Given all this, the seasonal distributions
394 of PAHs sources indicated that the pollution of atmospheric PAHs was mainly influenced by human
395 activities.



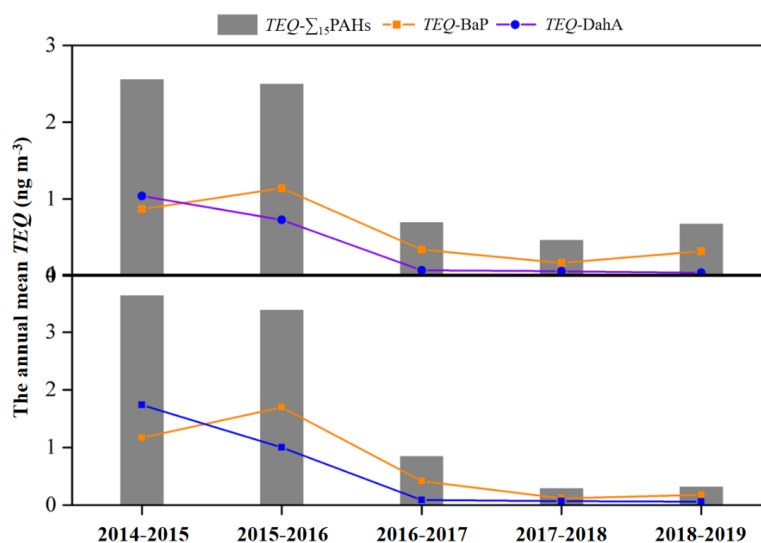
396 3.3 Health risk exposed to PAHs

397 On the basis of the Eq. (3), the annual mean *TEQ* value around the BS was $1.37 \pm 1.05 \text{ ng m}^{-3}$
398 ³ from June 2014 to May 2019, which below the national standard (10 ng m^{-3}) while slightly higher
399 than the WHO standard (1 ng m^{-3}). The HMW-PAHs contributed dominantly 76.4% of the total
400 *TEQ*. However, the concentration of HMW-PAHs in the atmosphere accounted for 6.5% of the total
401 PAH concentration. Among which, the two major *TEQ* contributors were BaP ($38.2\% \pm 8.0\%$) and
402 DahA ($16.6\% \pm 9.0\%$). For TJ, the annual mean *TEQ* value was $1.69 \pm 1.50 \text{ ng m}^{-3}$, which was
403 slightly higher than that the BS. It was indicating that higher health risk was caused by PAHs
404 exposed at TJ than around the BS. The HMW-PAHs contributed dominantly 90.9% of the total
405 *TEQ*. However, the concentration of HMW-PAHs in the atmosphere accounted for 8% of total
406 PAHs concentrations. Among which, the two major contributors were BaP ($47.2\% \pm 9.2\%$) and
407 DahA ($19.7\% \pm 16.2\%$).

408 The information of *TEQ* at BS and TJ from June 2014 to May 2019 was shown in Figure 5.
409 The average value of *TEQ* at the BS in the five cycle years was $2.55 \pm 1.49 \text{ ng m}^{-3}$, $2.49 \pm 1.63 \text{ ng m}^{-3}$,
410 $0.69 \pm 0.76 \text{ ng m}^{-3}$, $0.47 \pm 0.66 \text{ ng m}^{-3}$, and $0.67 \pm 0.84 \text{ ng m}^{-3}$, respectively. The value of *TEQ*
411 at the BS showed a downward trend year by year. The decrease in the fifth year compared with the
412 first year was more than two times, indicating that the environmental health risk of PAHs was
413 decreasing. It was found that the decrease of HMW-PAHs concentration was the main reason for
414 the decrease of the toxicity of PAHs. For example, the concentration of BaP in the atmosphere at
415 the BS decreased by 79.1% in five years, and the concentration of DahA, as a species with
416 carcinogenic toxicity equivalent to BaP, decreased by 96.1%. For TJ, the average value of *TEQ* in
417 the five cycle years was $3.63 \pm 0.14 \text{ ng m}^{-3}$, $3.38 \pm 0.72 \text{ ng m}^{-3}$, $0.84 \pm 0.38 \text{ ng m}^{-3}$, $0.28 \pm 0.10 \text{ ng m}^{-3}$,
418 and $0.31 \pm 0.15 \text{ ng m}^{-3}$, respectively. The *TEQ* value of PAHs in the atmosphere decreased by
419 91.5% at TJ in the past five years. At TJ, BaP and DahA as the major contributing factors of *TEQ*
420 in the atmosphere also showed more significant decline than around the BS. To sum up, the results
421 showed that pollution control could not only reduce the total concentration of PAHs in the
422 atmosphere at the BS, but also affected the composition of the PAHs. And it mainly affected the



423 concentration of HMW-PAHs compounds, which the total toxic equivalent of PAHs in the
424 atmosphere at the BS was remarkably reduced.
425



426 **Figure 5.** The annual mean *TEQ* of 15 PAHs, BaP, and DahA in the atmosphere at the BS (the
427 upper part) and TJ (the lower part) from June 2014 to May 2019.

428

429 Simultaneously, incremental lifetime cancer risk (*ILCR*) was used to assess the potential
430 carcinogenic risk of PAHs in the atmosphere at the BS. According to the USEPA, the *ILCR* value
431 less than 1×10^{-6} was an acceptable risk level. When the *ILCR* value was equal to or high than $1 \times$
432 10^{-6} but less than 1×10^{-4} , which was in a serious risk of cancer, and health issues should be taken
433 seriously. When the *ILCR* value were equal to or greater than 1×10^{-4} , it was considered life-
434 threatening for human. The specific calculation was seen Eq. (4). It was found that the range of
435 *ILCR* value of atmospheric PAHs at the BS region for five years was 4.1×10^{-5} – 2.2×10^{-4} , with an
436 average value of 1.2×10^{-4} , which means that the risk of cancer in this region was in a serious state,
437 and health problems should be paid more attention to. Similarly, to the above *TEQ*, *ILCR* values
438 were also dominated by HMW-PAHs. The *ILCR* caused by PAHs is listed in Table S14 of SI. The



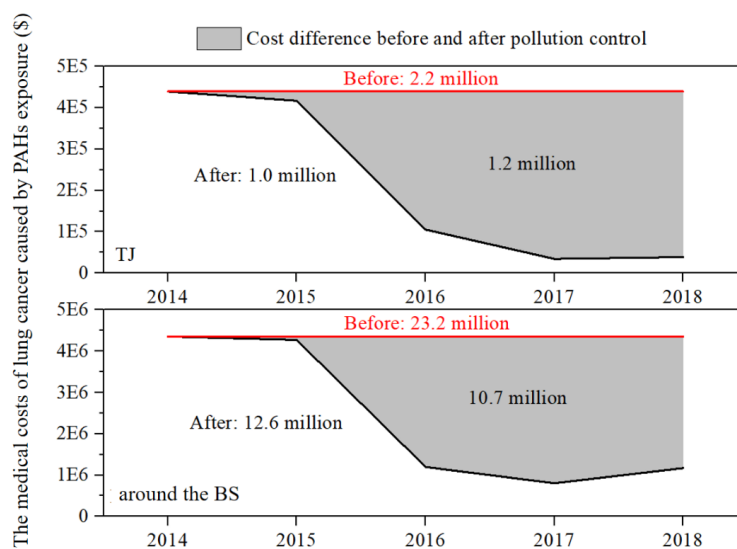
439 *ILCR* at the BS decreased significantly by 74.1% from 2.2×10^{-4} in the first year to 5.7×10^{-5} in
440 the fifth year. Compared with the BS, the *ILCR* at TJ decreased more significantly, from 3.2×10^{-4}
441 to 2.7×10^{-5} by 91.6%. As shown in Table S15 of SI, the study found that the concentration
442 variations of highly toxic BaP and DahA were basically synchronized with the changes of *ILCR*,
443 which implied that the decrease of concentrations of both was the main reason for the cancer risk
444 reduction. The significant reduction of cancer risk at the BS region indicated that the emission of
445 highly toxic HMW-PAHs in the atmosphere has been effectively controlled, which also reflected
446 that the prevention and control of air pollution had effectively reduced the health risk. In particular,
447 the reduction effect of PAHs exposure risk was more obvious at TJ, which air pollution control was
448 strict.

449 **3.4. Direct medical costs of lung cancer caused by exposed to PAHs**

450 This reduction of PAHs health risk would lead to a reduction in the number of people who
451 develop cancer, thus saving on the cost of cancer treatment. In this study, the direct medical costs
452 of lung cancer caused by respiratory exposure to PAHs was estimated by the additional incidence
453 of lung cancer caused by PAHs exposure, the population in the study area, and the direct medical
454 costs per capita of lung cancer patients. The specific calculation was seen Eq. (5). In addition to
455 PAHs exposure, there were many environmental risk factors that could induce lung cancer. For
456 deriving the lung cancer burden caused by atmospheric PAHs respiratory exposure from the
457 incidence of lung cancer, this study was characterized by percentage of population risk attribution
458 (*PAF*). The details were seen Eq. (6) and Eq. (7). *PAF* here represented the percentage of reduction
459 in lung cancer incidence which PAHs, an environmental factor, were completely removed or their
460 concentration was reduced. According to the above introduction of *PAF* and analysis of *TEQ*, the
461 directly calculated *PAF* within five years around the BS ranged from 0.5‰ to 2.7‰, with an
462 average value of 1.4‰. The five-year *PAF* at TJ ranged from 0.3‰ to 3.8‰, with an average value
463 of 1.7‰. A remarkable situation was that *PAF* around the BS region and TJ decreased significantly
464 in the past five years, from 3.8‰ and 2.7‰ in the first year to 0.3‰ and 0.7‰ in the fifth year
465 respectively. The additional lung cancer incidence (I_{add}) due to respiratory exposure to PAHs was



466 calculated using the product of lung cancer incidence and *PAF*. Previous studies reported that the
467 incidence of lung cancer at TJ in 2012 was 87.37×10^{-5} (Cao et al., 2016). In this study, $87.37 \times$
468 10^{-5} was used as the reference value of lung cancer incidence. The average I_{add} caused by
469 respiratory exposure to PAHs around the BS region and TJ were 1.26×10^{-6} and 1.55×10^{-6} ,
470 respectively. During the observation of the five-year, the I_{add} around the BS region and TJ decreased
471 from 2.34×10^{-6} and 3.33×10^{-6} in the first year to 6.15×10^{-7} and 2.87×10^{-7} in the fifth year,
472 respectively. The population numbers in the study area were all referred from the public data of the
473 statistical yearbook. The estimated results of the BS region and TJ are shown in Table S16–S17 of
474 SI, respectively. It had been reported that the direct cost of an average case of lung cancer patients
475 in China in 2014 was \$9042.79 (Shi et al., 2017; Huang et al., 2016). Since there was no reference
476 data available for other corresponding years, this study took the direct cost per case of lung cancer
477 patients as the baseline in 2014, and the estimate assumed the same direct medical costs per capita
478 for lung cancer within five years.
479



480 **Figure 6.** The medical costs of lung cancer caused by PAHs exposure before and after the control
481 of air pollution at TJ and around the BS from 2014 to 2018.



482

483 Figure 6 shows the comparative results of direct medical costs of lung cancer at the BS region
484 and TJ under two scenarios from 2014 to 2018. In the five years, under the implementation of air
485 pollution control, the total direct medical costs of lung cancer caused by respiratory exposure to
486 PAHs in the Bohai Rim region was \$12.6 million. Assuming that no air pollution control was
487 implemented, the total direct medical costs of lung cancer caused by PAHs exposure did not change
488 in five years, and the total direct medical costs was five times in 2014 with an estimated value of
489 \$23.2 million. The actual implementation of control on the total direct medical costs of lung cancer
490 saved \$10.7 million. At TJ, the total direct medical costs of lung cancer induced by respiratory
491 exposure to PAHs under actual air pollution control was \$1.0 million. Under the assumption that
492 no air pollution control was implemented, the total direct medical costs of lung cancer caused by
493 PAHs exposure was \$2.2 million, saving about \$1.2 million at TJ. Compared to without air
494 pollution control, the total direct medical costs of lung cancer caused by PAHs exposure decreased
495 by 46.1% around the BS region and by an even greater 54.5% at TJ. This illustrated that the
496 implementation of air pollution control not only reduced the risk of lung cancer caused by PAHs
497 exposure around the BS region, but also created significant health benefit in the direct medical
498 costs of lung cancer, especially in tightly controlled areas such as TJ. Therefore, the above results
499 noted that more precise pollution prevention and control could better reduce the emission of the
500 pollutants, and sequentially reduce the health risk of human expose.

501

502 **4 Conclusions**

503 A five-year atmospheric PAHs observation was conducted at twelve sites around the BS from
504 June 2014 to May 2019. The five-year atmospheric concentration of $\Sigma_{15}\text{PAHs}$ was $56.8 \pm 8.4 \text{ ng m}^{-3}$,
505 characterized by dominant LMW-PAHs ($58.7 \pm 7.8\%$). The maximum annual concentrations and
506 seasonal concentrations occurred in the first year and every winter, respectively. The concentrations
507 of $\Sigma_{15}\text{PAHs}$ in the atmosphere reduced significantly around the BS, especially at the sampling site
508 of TJ during the sampling period. The contributions of coal combustion and vehicle emission to



509 PAHs in the atmosphere during the sampling period showed an increase and a decrease around the
510 BS, respectively. However, the variations of coal combustion and vehicle emission in the source
511 contributions in TJ were just the opposite. From 2014 to 2018, the additional lung cancer incidence
512 of lung cancer caused by PAH exposure around the BS dropped by 74.1%, and a higher drop of
513 91.6% in TJ. From the statistical standpoint, the drop of the incidence saved about \$10.7 million
514 for the total direct medical costs of lung cancer caused by PAHs exposure around the BS. Compared
515 to without air pollution control, the total direct medical costs of lung cancer caused by PAHs
516 exposure decreased by 46.1% around the BS region and by an even greater 54.5% at TJ. And it was
517 further be certified that pollution reduction was beneficial to human health. In the fight against air
518 pollution, more precise pollution prevention and control strategies were needed.

519

520 **Data availability.** Corresponding data for the samples can be accessed on request to the
521 corresponding author (Chongguo Tian, cgtian@yic.ac.cn)

522

523 **Author contributions.** CT and ZZ designed the research; WM, RS, XW, ZZ, ZS, and CT
524 conducted the sample collection; WM, RS, and XW performed the chemical analyses; WM, RS,
525 XW, and CT analyzed the data, carried out the simulations and wrote the original article; ZS, SZ,
526 JT, SC, JL, and GZ helped with article submissions. All authors have given approval to the final
527 version of the manuscript.

528

529 **Competing interests.** The contact author has declared that none of the authors has any competing
530 interests.

531

532 **Acknowledgements.** This study was supported by the National Natural Science Foundation of
533 China (No. 41977190 and 42177089).

534

535 **Reference**



536 Air quality historical data query: <https://www.aqistudy.cn/historydata/>, last access: 31 August 2023,
537 [2014-2019](https://doi.org/10.1016/j.scitotenv.2017.03.256).

538 Alves, C.A., Vicente, A.M., Custodio, D., Cerqueira, M., Nunes, T., Pio, C., Lucarelli, F., Calzolari,
539 G., Nava, S., Diapouli, E., Eleftheriadis, K., Querol, X., and Musa Bandowe, B.A.: Polycyclic
540 aromatic hydrocarbons and their derivatives (nitro-PAHs, oxygenated PAHs, and azaarenes) in
541 PM_{2.5} from Southern European cities, *Sci. Total. Environ.*, 595, 494–504,
542 <https://doi.org/10.1016/j.scitotenv.2017.03.256>, 2017.

543 Bai, Z.P., Hu, Y.D., Yu, H., Wu, N., and You, Y.: Quantitative health risk assessment of inhalation
544 exposure to polycyclic aromatic hydrocarbons on citizens in Tianjin, China, *B. Environ. Contam.*
545 *Tox.*, 83, 151–154, <https://doi.org/10.1007/s00128-009-9686-8>, 2009.

546 Biache, C., Mansuy-Huault, L., and Faure, P.: Impact of oxidation and biodegradation on the most
547 commonly used polycyclic aromatic hydrocarbon (PAH) diagnostic ratios: Implications for the
548 source identifications, *J. Hazard. Mater.*, 267, 31–39,
549 <https://doi.org/10.1016/j.jhazmat.2013.12.036>, 2014.

550 Bulletin of the State of China's ecological Environment:
551 <http://www.mee.gov.cn/hjzl/sthjzk/zghjzkgb/>, last access: 31 August 2023, 2021.

552 Cao, M., Wang, M., and Song, F.: Secular trend of lung cancer incidence in Hexi District, Tianjin,
553 1992 – 2012, *Tumor.*, 36, 1330–1334, <https://doi.org/10.3781/j.issn.1000-7431.2016.22.553>, 2016.

554 Chao, S.H., Liu, J.W., Chen, Y.J., Cao, H.B., and Zhang, A.C.: Implications of seasonal control of
555 PM_{2.5}-bound PAHs: An integrated approach for source apportionment, source region identification
556 and health risk assessment, *Environ. Pollut.*, 247, 685–695,
557 <https://doi.org/10.1016/j.envpol.2018.12.074>, 2019.

558 Chen, C., Fang, J.L., Shi, W.Y., Li, T.T., and Shi, X.M.: Clean air actions and health plans in China,
559 *Chinese Medical Journal.*, 133, 1609–1611, <https://doi.org/10.1097/cm9.0000000000000888>,
560 2020.



- 561 Colvin, K.A., Lewis, C., and Galloway, T.S.: Current issues confounding the rapid toxicological
562 assessment of oil spills, *Chemosphere.*, 245, 125585,
563 <https://doi.org/10.1016/j.chemosphere.2019.125585>, 2020.
- 564 Ding, Y.H., and Chan, J.C.L.: The East Asian summer monsoon: an overview, *Meteorol. Atmos.*
565 *Phys.*, 89, 117–142, <https://doi.org/10.1007/s00703-005-0125-z>, 2005.
- 566 Eng, A., Harner, T., and Pozo, K.: A prototype passive air sampler for measuring dry deposition of
567 polycyclic aromatic hydrocarbons, *Environ. Sci. Technol. Let.*, 1, 77–81,
568 <https://doi.org/10.1021/ez400044z>, 2014.
- 569 Fan, L.P., Fu, S., Wang, X., Fu, Q.Y., Jia, H.H., Xu, H., Qin, G.M., Hu, X., and Cheng, J.P.:
570 Spatiotemporal variations of ambient air pollutants and meteorological influences over typical
571 urban agglomerations in China during the COVID-19 lockdown, *J. ENVIRON. SCI.*, 106, 26–38,
572 <https://doi.org/10.1016/j.jes.2021.01.006>, 2021.
- 573 Fang, D., Wang, Q., Li, H., Yu, Y., Lu, Y., and Qian, X.: Mortality effects assessment of ambient
574 PM_{2.5} pollution in the 74 leading cities of China, *Sci. Total. Environ.*, 569-570, 1545–1552,
575 <https://doi.org/10.1016/j.scitotenv.2016.06.248>, 2016.
- 576 Fang, Y., Chen, Y., Tian, C., Lin, T., Hu, L., Li, J., Zhang, G.: Application of PMF receptor model
577 merging with PAHs signatures for source apportionment of black carbon in the continental shelf
578 surface sediments of the Bohai and Yellow Seas, China, *J. Geophys. Res-Oceans.*, 121, 1346–1359,
579 <https://doi.org/10.1002/2015JC011214>, 2016.
- 580 Feng, J., Guo, Z., Chan, C.K., and Fang, M.: Properties of organic matter in PM_{2.5} at Changdao
581 Island, China - A rural site in the transport path of the Asian continental outflow, *Atmos. Environ.*,
582 41, 1924–1935, <https://doi.org/10.1016/j.atmosenv.2006.10.064>, 2007.
- 583 Gao, Y., Guo, X., Ji, H., Li, C., Ding, H., Briki, M., Tang, L., and Zhang, Y.: Potential threat of
584 heavy metals and PAHs in PM_{2.5} in different urban functional areas of Beijing, *Atmos. Res.*, 178-
585 179, 6–16, <https://doi.org/10.1016/j.atmosres.2016.03.015>, 2016.



- 586 Gibbs, G.W.: Estimating residential polycyclic aromatic hydrocarbon (PAH) related lung cancer
587 risks using occupational data, *The Annals of Occupational Hygiene.*, 41, 49–53,
588 https://doi.org/10.1093/ANNHYG/41.INHALED_PARTICLES_VIII.49, 1997.
- 589 Gong, P., Wang, X.P., and Yao, T.D.: Ambient distribution of particulate- and gas-phase n-alkanes
590 and polycyclic aromatic hydrocarbons in the Tibetan Plateau, *Environ. Earth. Sci.*, 64, 1703–1711,
591 <https://doi.org/10.1007/s12665-011-0974-3>, 2011.
- 592 Guo, X., Zhao, L., Chen, D., Jia, Y., Zhao, N., Liu, W., and Cheng, S.: Air quality improvement
593 and health benefit of PM_{2.5} reduction from the coal cap policy in the Beijing-Tianjin-Hebei (BTH)
594 region, China, *Environ. Sci. Pollut. R.*, 25, 32709–32720, [https://doi.org/10.1007/s11356-018-](https://doi.org/10.1007/s11356-018-3014-y)
595 [3014-y](https://doi.org/10.1007/s11356-018-3014-y), 2018.
- 596 Han, M., Liu, S., Liu, M., Lu, M., Yan, W., He, Y., Dang, H., Dai, X., Zhang, Z., Du, X., and Meng,
597 F.: Assessment of the effect of the reduction of the residential coal combustion on the atmospheric
598 BaP pollution in Beijing-Tianjin-Hebei region, *China Environmental Science.*, 38, 3262–3272,
599 <https://doi.org/10.19674/j.cnki.issn1000-6923.2018.0350-en>, 2018.
- 600 Hong, W.J., Jia, H., Ma, W.L., Sinha, R.K., Moon, H.B., Nakata, H., Nguyen Hung, M., Chi, K.H.,
601 Li, W.L., Kannan, K., Sverko, E., and Li, Y.F.: Distribution, fate, inhalation exposure and lung
602 cancer risk of atmospheric polycyclic aromatic hydrocarbons in some Asian countries, *Environ.*
603 *Sci. Technol.*, 50, 7163–7174, <https://doi.org/10.1021/acs.est.6b01090>, 2016.
- 604 Huang, C., Wang, Q., Wang, S., Ren, M., Ma, R., and He, Y.: Air pollution prevention and control
605 policy in China, *Adv. Exp. Med. Biol.*, 1017, 243–261, [https://doi.org/10.1007/978-981-10-5657-](https://doi.org/10.1007/978-981-10-5657-4_11)
606 [4_11](https://doi.org/10.1007/978-981-10-5657-4_11), 2017.
- 607 Huang, H.Y., Shi, J.F., Guo, L.W., Zhu, X.Y., Wang, L., Liao, X.Z., Liu, G.X., Bai, Y.N., Mao, A.Y.,
608 Ren, J.S., Sun, X.J., Zhang, K., He, J., Dai, M.: Expenditure and financial burden for common
609 cancers in China: a hospital-based multicentre cross-sectional study, *Lancet.*, 388, 10–10,
610 [https://doi.org/10.1016/S0140-6736\(16\)31937-7](https://doi.org/10.1016/S0140-6736(16)31937-7), 2016.
- 611 Jaward, T.M., Zhang, G., Nam, J.J., Sweetman, A.J., Obbard, J.P., Kobara, Y., and Jones, K.C.:
612 Passive air sampling of polychlorinated biphenyls, organochlorine compounds, and



613 polybrominated diphenyl ethers across Asia, *Environ. Sci. Technol.*, 39, 8638–8645,
614 <https://doi.org/10.1021/es051382h>, 2005.

615 Jia, Y.L., Stone, D., Wang, W.T., Schrlau, J., Tao, S., and Simonich, S.L.M.: Estimated reduction in
616 cancer risk due to PAH exposures if source control measures during the 2008 Beijing Olympics
617 were sustained, *Environ. Health. Persp.*, 119, 815–820, <https://doi.org/10.1289/ehp.1003100>, 2011.

618 Li, N., Zhang, X., Shi, M., and Hewings, G.J.D.: Does China's air pollution abatement policy matter?
619 An assessment of the Beijing-Tianjin-Hebei region based on a multi-regional CGE model, *Energ.*
620 *Policy.*, 127, 213–227, <https://doi.org/10.1016/j.enpol.2018.12.019>, 2019.

621 Li, W., Park, R., Alexandrou, N., Dryfhout-Clark, H., Brice, K., and Hung, H.: Multi-year analyses
622 reveal different trends, sources, and implications for source-related human health risks of
623 atmospheric polycyclic aromatic hydrocarbons in the Canadian Great Lakes Basin, *Environ. Sci.*
624 *Technol.*, 55, 2254–2264, <https://doi.org/10.1021/acs.est.0c07079>, 2021.

625 Li, Z.Y., Wang, Y.T., Li, Z.X., Guo, S.T., and Hu, Y.: Levels and Sources of PM_{2.5}-associated PAHs
626 during and after the Wheat Harvest in a Central Rural Area of the Beijing-Tianjin-Hebei (BTH)
627 Region, *Aerosol. Air. Qual. Res.*, 20, 1070–1082, <https://doi.org/10.4209/aaqr.2020.03.0083>, 2020.

628 Lian, L., Huang, T., Ling, Z., Li, S., Li, J., Jiang, W., Gao, H., Tao, S., Liu, J., Xie, Z., Mao, X.,
629 Ma, J.: Interprovincial trade driven relocation of polycyclic aromatic hydrocarbons and lung cancer
630 risk in China, *J. Clean. Prod.*, 280, 124368, <https://doi.org/10.1016/j.jclepro.2020.124368>, 2021.

631 Lin, Y., Ma, Y., Qiu, X., Li, R., Fang, Y., Wang, J., Zhu, Y., and Hu, D.: Sources, transformation,
632 and health implications of PAHs and their nitrated, hydroxylated, and oxygenated derivatives in
633 PM_{2.5} in Beijing, *Journal of Geophysical Research.*, 120, 7219–7228,
634 <https://doi.org/10.1002/2015JD023628>, 2015.

635 Liu, H., Li, B., Qi, H., Ma, L., Xu, J., Wang, M., Ma, W., and Tian, C.: Source apportionment and
636 toxic potency of polycyclic aromatic hydrocarbons (PAHs) in the air of Harbin, a cold city in
637 Northern China, *Atmosphere-Basel.*, 12, <https://doi.org/10.3390/atmos12030297>, 2021.



- 638 Liu, L., Zhen, X., Wang, X., Li, Y., Sun, X., and Tang, J.: Legacy and novel halogenated flame
639 retardants in seawater and atmosphere of the BS: Spatial trends, seasonal variations, and
640 influencing factors, *Water. Res.*, 184, <https://doi.org/10.1016/j.watres.2020.116117>, 2020.
- 641 Liu, W.J., Xu, Y.S., Zhao, Y.Z., Liu, Q.Y., Yu, S.Y., Liu, Y., Wang, X., Liu, Y., Tao, S., and Liu,
642 W.X.: Occurrence, source, and risk assessment of atmospheric parent polycyclic aromatic
643 hydrocarbons in the coastal cities of the Bohai and Yellow Seas, China, *Environ. Pollut.*, 254,
644 <https://doi.org/10.1016/j.envpol.2019.113046>, 2019.
- 645 Luo, M., Ji, Y.Y., Ren, Y.Q., Gao, F.H., Zhang, H., Zhang, L.H., Yu, Y.Q., and Li, H.: Characteristics
646 and health risk assessment of PM_{2.5}-bound PAHs during heavy air pollution episodes in winter in
647 urban area of Beijing, China, *Atmosphere-Basel.*, 12, 323, <https://doi.org/10.3390/atmos12030323>,
648 2021.
- 649 Lv, Min., Luan, Xiaolin., Liao, Chunyang., Wang, Dongqi., Liu, Dongyan., Zhang, Gan., Jiang,
650 Guibin., Chen, Lingxin.: Human impacts on polycyclic aromatic hydrocarbon distribution in
651 Chinese intertidal zones, *Nature Sustainability.*, <https://doi.org/10.1038/s41893-020-0565-y>, 2020.
- 652 Ma, W.L., Li, Y.F., Qi, H., Sun, D.Z., Liu, L.Y., and Wang, D.G.: Seasonal variations of sources of
653 polycyclic aromatic hydrocarbons (PAHs) to a northeastern urban city, China, *Chemosphere.*, 79,
654 441–447, <https://doi.org/10.1016/j.chemosphere.2010.01.048>, 2010.
- 655 Ma, W.L., Liu, L.Y., Jia, H.L., Yang, M., and Li, Y.F.: PAHs in Chinese atmosphere Part I:
656 Concentration, source and temperature dependence, *Atmos. Environ.*, 173, 330–337,
657 <https://doi.org/10.1016/j.atmosenv.2017.11.029>, 2018.
- 658 Ma, W.L., Zhu, F.J., Liu, L.Y., Jia, H.L., Yang, M., and Li, Y.F.: PAHs in Chinese atmosphere Part
659 II: Health risk assessment, *Ecotox. Environ. Safe.*, 200, 110774,
660 <https://doi.org/10.1016/j.ecoenv.2020.110774>, 2020.
- 661 Ma, Y.X., Xie, Z.Y., Yang, H.Z., Moller, A., Halsall, C., Cai, M.H., Sturm, R., and Ebinghaus, R.:
662 Deposition of polycyclic aromatic hydrocarbons in the North Pacific and the Arctic, *J. Geophys.*
663 *Res-Atmos.*, 118, 5822–5829, <https://doi.org/10.1002/jgrd.50473>, 2013.



- 664 Marvin, C.H., Tomy, G.T., Thomas, P.J., Holloway, A.C., Sandau, C.D., Idowu, I., and Xia, Z.:
665 Considerations for prioritization of polycyclic aromatic compounds as environmental contaminants,
666 *Environ. Sci. Technol.*, 54, 14787–14789, <https://doi.org/10.1021/acs.est.0c04892>, 2020.
- 667 Menzler, S., Piller, G., Gruson, M., Rosario, A.S., Wichmann, H.E., and Kreienbrock, L.:
668 Population attributable fraction for lung cancer due to residential radon in Switzerland and
669 Germany, *Health. Phys.*, 95, 179–189, <https://doi.org/10.1097/01.Hp.0000309769.55126.03>, 2008.
- 670 Moeckel, C., Harner, T., Nizzetto, L., Strandberg, B., Lindroth, A., and Jones, K.C.: Use of
671 depuration compounds in passive air samplers: results from active sampling-supported field
672 deployment, potential uses, and recommendations, *Environ. Sci. Technol.*, 43, 3227–3232,
673 <https://doi.org/10.1021/es802897x>, 2009.
- 674 Paatero, P., Eberly, S., Brown, S.G., and Norris, G.A.: Methods for estimating uncertainty in factor
675 analytic solutions, *Atmos. Meas. Tech.*, 7, 781–797, <https://doi.org/10.5194/amt-7-781-2014>, 2014.
- 676 Qin, F., Liu, H.Y., Jing, L., Liu, W., Yin, J., and Wei, X.D.: The investigation of energy consumption
677 in the village of Jilin province, *Journal of Jilin Jianzhu University (China)*, 2, 37–40,
678 <https://d.wanfangdata.com.cn/periodical/jljzgcxyxb200702011>, 2007.
- 679 Qu, L., Yang, L., Zhang, Y., Wang, X., Sun, R., Li, B., Lv, X., Chen, Y., Wang, Q., Tian, C., and Ji,
680 L.: Source Apportionment and Toxic Potency of PM_{2.5}-Bound Polycyclic Aromatic Hydrocarbons
681 (PAHs) at an Island in the Middle of Bohai Sea, China, *Atmosphere*, 13,
682 <https://doi.org/10.3390/atmos13050699>, 2022.
- 683 Shi, C.L., Lou, P.A., Shi, J.F., Huang, H.Y., Li, J., Yue, Y.P., Wang, L., Dong, Z.M., Chen, P.P.,
684 Zhang, P., Zhao, C.Y., Li, F., Zhou, J.Y., and Dai, M.: Economic burden of lung cancer in mainland
685 China, 1996–2014: a systematic review, *China Journal of Public Health*, 33, 1767–1774,
686 <https://doi.org/10.11847/zgggws2017-33-12-25>, 2017.
- 687 Sofowote, U.M., Hung, H., Rastogi, A.K., Westgate, J.N., Deluca, P.F., Su, Y.S., and McCarry, B.E.:
688 Assessing the long-range transport of PAH to a sub-Arctic site using positive matrix factorization
689 and potential source contribution function, *Atmos. Environ.*, 45, 967–976,
690 <https://doi.org/10.1016/j.atmosenv.2010.11.005>, 2011.



691 Sun, R., Wang, X., Tian, C., Zong, Z., Ma, W., Zhao, S., Wang, Y., Tang, J., Cui, S., Li, J., and
692 Zhang, G.: Exploring source footprint of Organophosphate esters in the Bohai Sea, China: Insight
693 from temporal and spatial variabilities in the atmosphere from June 2014 to May 2019, *Environ.*
694 *Int.*, 159, <https://doi.org/10.1016/j.envint.2021.107044>, 2022.

695 Tan, J.H., Bi, X.H., Duan, J.C., Rahn, Kenneth A., Sheng, G.Y., and Fu, J.M.: Seasonal variation
696 of particulate polycyclic aromatic hydrocarbons associated with PM₁₀ in Guangzhou, China, *Atmos.*
697 *Res.*, 80, 250–262, <https://doi.org/10.1016/j.atmosres.2005.09.004>, 2006.

698 Tian, C., Ma, J., Liu, L., Jia, H., Xu, D., and Li, Y.F.: A modeling assessment of association between
699 East Asian summer monsoon and fate/outflow of α -HCH in Northeast Asia, *Atmos. Environ.*, 43,
700 3891-3901, <https://doi.org/https://doi.org/10.1016/j.atmosenv.2009.04.056>, 2009.

701 Tong, L., Peng, C.H., Huang, Z.W., Zhang, J.J., Dai, X.R., Xiao, H., Xu, N.B., and He, J.:
702 Identifying the pollution characteristics of atmospheric polycyclic aromatic hydrocarbons
703 associated with functional districts in Ningbo, China, *B. Environ. Contam. Tox.*, 103, 34–40,
704 <https://doi.org/10.1007/s00128-018-02535-4>, 2019.

705 Wang, X.P., Zong, Z., Tian, C.G., Chen, Y.J., Luo, C.L., Tang, J.H., Li, J., Zhang, G.: Assessing on
706 toxic potency of PM_{2.5}-bound polycyclic aromatic hydrocarbons at a national atmospheric
707 background site in North China, *Sci. Total. Environ.*, 612, 330–338,
708 <https://doi.org/10.1016/j.scitotenv.2017.08.208>, 2018.

709 Wu, D., Xu, Y., and Zhang, S.: Will joint regional air pollution control be more cost-effective? An
710 empirical study of China's Beijing-Tianjin-Hebei region, *J. Environ. Manage.*, 149, 27–36,
711 <https://doi.org/10.1016/j.jenvman.2014.09.032>, 2015.

712 Xing, X., Chen, Z., Tian, Q., Mao, Y., Liu, W., Shi, M., Cheng, C., Hu, T., Zhu, G., Li, Y., Zheng,
713 H., Zhang, J., Kong, S., and Qi, S.: Characterization and source identification of PM_{2.5}-bound
714 polycyclic aromatic hydrocarbons in urban, suburban, and rural ambient air, central China during
715 summer harvest, *Ecotox. Environ. Safe.*, 191, <https://doi.org/10.1016/j.ecoenv.2020.110219>, 2020.

716 Yan, Z., Jin, L., Chen, X., Wang, H., Tang, Q., Wang, L., and Lei, Y.: Assessment of air pollutants
717 emission reduction potential and health benefits for residential heating coal changing to electricity



718 in the Beijing-Tianjin-Hebei region, *Research of Environmental Sciences.*, 32, 95–103,
719 <https://doi.org/10.13198/j.issn.1001-6929.2018.10.16>, 2019.

720 Yang, Q.Q., Yuan, Q.Q., Li, T.W., Shen, H.F., and Zhang, L.P.: The relationships between PM_{2.5}
721 and meteorological factors in China: seasonal and regional variations, *Int. J. Env. Res. Pub. He.*,
722 14, <https://doi.org/10.3390/ijerph14121510>, 2017.

723 Yu, Q.Q., Gao, B., Li, G.H., Zhang, Y.L., He, Q.F., Deng, W., Huang, Z.H., Ding, X., Hu, Q.H.,
724 Huang, Z.Z., Wang, Y.J., Bi, X.H., and Wang, X.M.: Attributing risk burden of PM_{2.5}-bound
725 polycyclic aromatic hydrocarbons to major emission sources: Case study in Guangzhou, south
726 China, *Atmos. Environ.*, 142, 313–323, <https://doi.org/10.1016/j.atmosenv.2016.08.009>, 2016.

727 Zhang, J., Liu, W., Xu, Y., Cai, C., Liu, Y., Tao, S., and Liu, W.: Distribution characteristics of and
728 personal exposure with polycyclic aromatic hydrocarbons and particulate matter in indoor and
729 outdoor air of rural households in Northern China, *Environ. Pollut.*, 255, 113176,
730 <https://doi.org/10.1016/j.envpol.2019.113176>, 2019.

731 Zhang, J.W., Feng, L.H., Zhao, Y., Hou, C.C., and Gu, Q.: Health risks of PM_{2.5}-bound polycyclic
732 aromatic hydrocarbon (PAH) and heavy metals (PPAH&HM) during the replacement of central
733 heating with urban natural gas in Tianjin, China, *Environ. Geochem. Hlth.*, 44, 2495–2514,
734 <https://doi.org/10.1007/s10653-021-01040-8>, 2021.

735 Zhang, J.W., Zhao, J., Cai, J., Gao, S.T., Li, J., Zeng, X.Y., and Yu, Z.Q.: Spatial distribution and
736 source apportionment of atmospheric polycyclic aromatic hydrocarbons in the Pearl River Delta,
737 China, *Atmos. Pollut. Res.*, 9, 887–893, <https://doi.org/10.1016/j.apr.2018.02.004>, 2018.

738 Zhang, S.W., Chen, W.Q., Kong, L.Z., Li, G.L., and Zhao, P.: An Annual Report: Cancer Incidence
739 in 35 Cancer Registries in China, 2003, *China Cancer.*, 494–507,
740 <https://doi.org/10.3969/j.issn.1004-0242.2007.07.001>, 2007.

741 Zhang, Y.J., Lin, Y., Cai, J., Liu, Y., Hong, L.N., Qin, M.M., Zhao, Y.F., Ma, J., Wang, X.S., Zhu,
742 T., Qiu, X.H., and Zheng, M.: Atmospheric PAHs in North China: Spatial distribution and sources,
743 *Sci. Total. Environ.*, 565, 994–1000, <https://doi.org/10.1016/j.scitotenv.2016.05.104>, 2016.



744 Zhang, Y.X., Tao, S., Cao, J., and Coveney, R.M.: Emission of polycyclic aromatic hydrocarbons
745 in China by county, *Environ. Sci. Technol.*, 41, 683–687, <https://doi.org/10.1021/es061545h>, 2007.
746 Zhang, Y.X., Tao, S., Shen, H.Z., and Ma, J.M.: Inhalation exposure to ambient polycyclic aromatic
747 hydrocarbons and lung cancer risk of Chinese population, *P. Natl. Acad. Sci. USA.*, 106,
748 21063–21067, <https://doi.org/10.1073/pnas.0905756106>, 2009.
749 Zhao, H., Wu, R., Liu, Y., Cheng, J., Geng, G., Zheng, Y., Tian, H., He, K., and Zhang, Q.: Air
750 pollution health burden embodied in China's supply chains, *Environmental Science and*
751 *Ecotechnology.*, 16, 100264–100264, <https://doi.org/10.1016/j.ese.2023.100264>, 2023.
752 Zhi, Z., Wang, W., Cheng, M., Liu, S., Xu, J., He, Y., and Meng, F.: The contribution of residential
753 coal combustion to PM_{2.5} pollution over China's Beijing-Tianjin-Hebei region in winter, *Atmos.*
754 *Environ.*, 159, 147–161, <https://doi.org/10.1016/j.atmosenv.2017.03.054>, 2017.
755 Zhuo, S., Shen, G., Zhu, Y., Du, W., Pan, X., Li, T., Han, Y., Li, B., Liu, J., Cheng, H., Xing, B.,
756 and Tao, S.: Source-oriented risk assessment of inhalation exposure to ambient polycyclic aromatic
757 hydrocarbons and contributions of non-priority isomers in urban Nanjing, a megacity located in
758 Yangtze River Delta, China, *Environ. Pollut.*, 224, 796–809,
759 <https://doi.org/10.1016/j.envpol.2017.01.039>, 2017.